



Evaporation and Combustion Characteristics of Biomass Vacuum Pyrolysis Oils.

M. Garcia - Pèrez^{1,5}, P. Lappas², P. Hughes², L. Dell², A. Chaala¹, D. Kretschmer³ and C. Roy^{1,4}

¹Chemical Engineering Department,
Université Laval, Québec,
Canada

²Energy Research Laboratories,
CANMET, Ottawa,
Canada

³Mechanical Engineering Department,
Université Laval, Québec,
Canada

⁴Now at Pyrovac International,
Québec, Canada

⁵Now at University of Georgia (See Below)

Corresponding Author:

Manuel Garcia - Pérez

**University of Georgia
Biological and Agricultural Engineering Department
Driftmier Engineering Center
Athens, GA, 30602
USA**

Phone: (706)-254-7704
FAX : (706)-542-8806
e-mail : mgarcia@engr.uga.edu

ABSTRACT

The evaporation behaviour at high heating rates of vacuum pyrolysis oils obtained from Softwood Bark Residue (SWBR) and from Hardwood Rich in Fibres (HWRF) was studied photographically at the CANMET laminar Entrained Flow Reactor (EFR). For low heating rates, the evaporation and combustion characteristics for each bio-oil were studied by observing the mass loss in pure nitrogen and in air using thermogravimetry. The bio-oil combustion process starts with the evaporation of light compounds followed by the pyrolysis of heavy fractions yielding charcoal. In the final step, the oxygen reacts with charcoal to yield ash. Tests in the EFR were performed using initial droplet diameters between 58 and 62 μm . These diameters fall within the range of sizes observed in SWBR bio-oil sprays. The droplets were generated in a piezo-electric droplet generator and injected into a quartz tube reactor placed inside the furnace. Two furnace wall temperatures (700 °C and 800 °C) were used during EFR experiments. For evaporation studies, the EFR was operated in an inert environment (using Ar) while for combustion studies various Ar-O₂ mixtures were used (O₂ concentration between 20 and 50 vol. %). The photographic results showed that the formation of bubbles inside bio-oil droplets was influenced by heat transfer rates. For the experimental conditions used, no micro-explosions were observed. The solid residues obtained at the furnace exit were collected and analysed by Scanning Electron Microscopy. Two different morphologies of residual particles were observed depending on the frequency of droplet generation: a) compact and mechanically resistant spheres obtained at low electrical pulse frequencies (less than 500 Hz) with typical diameters of 20-30 μm and b) fragile “glass like” cenospheres with thin walls and diameter between 60 and 90 μm obtained at higher droplet generation frequencies (more than 500 Hz).

Key Words:

Combustion, evaporation, droplets, bio-oils, pyrolysis.

INTRODUCTION

The development of technologies to use renewable energy is an important research subject due to the political and environmental consequences of using fossil fuels. Biomass is one of the most attractive renewable resources to produce chemicals and energy. The pyrolysis of biomass has been extensively investigated as an alternative to convert these materials into bio-oils, char and gas. Bio-oils (also called “pyrolysis oils”) can be potentially used as liquid fuels.

The production of bio-oils offers advantages over conventional biomass combustion and gasification. During pyrolysis the alkali and other mineral components of the biomass are predominately entrapped in the char residue. The resulting liquid bio-fuel can be fired at high efficiency in Diesel engines or gas turbines (Czernik and Bridgwater, 2004). Also, the liquid state of this fuel can make feasible the geographical separation between the pyrolysis plant (close to the biomass sources) and the power units (close to the electricity consumers).

Using biofuels in gas turbine is not an easy task since the residence time of most gas turbines is very small (often less than 10 ms). Bio-oils have lower flame temperatures than petroleum-derived fuels and, therefore, a lower primary zone temperature, as well as an inferior volatility and a higher tendency to form a solid carbonaceous residue. Bio-oil droplets require considerably more time than conventional fuels to burn completely. Consequently, it is necessary to use higher residence times and different temperature and oxygen distributions in the combustion chambers in order to ensure complete combustion. The combustion chamber length must be proportional to the initial droplet radius of the largest droplet. If the droplet cannot be burned inside the combustion chamber, serious incrustation and erosion problems can arise and the level of particles in the exhaust stack may rise. Designers know how to estimate the burning time of petroleum-derived fuels and thus can determine the maximum permissible droplet-size and the desired Sauter Mean Diameter (SMD) of fuel sprays to assure a complete combustion. On the other hand, bio-oil evaporation and combustion kinetics is an

intensive research topic (Shaddix and Hardesty, 1996, Beer et al, 1994, Shaddix and Tennison, 1998, Wornat, Porter and Yang, 1994, Vitolo and Ghetti, 1994, D’Alessio et al, 1998, Calabria et al, 2000, Branca, DiBlasi and Elefante, 2004, Hallet, Clark and White, 2003).

Bio-oil droplet combustion studies have been reported over the last decade (Table 1). In these studies bio-oil evaporation and combustion were investigated by thermogravimetric techniques, in fibre-suspended droplets and in entrained flow reactors (EFR).

Research Centre	Observations	Ref.
ENTRAINED FLOW REACTORS		
Sandia, Livermore, California	Droplet furnace reactor. Temperatures (1600 K). Atmospheric pressure. Initial droplet size (320 µm). Oxygen concentrations (14-33 mol. %). Droplets generated at 16 Hz.	(Shaddix, Tennison, 1998) (Wornat, Porter, Yang, 1994)
Instituto Motori, Naples, Italy	Droplet furnace reactor. Temperatures (573 - 1123 K). Atmospheric pressure. Initial droplet size (50-100 µm). Tests carried out in nitrogen. Droplets generated by a Berglund-Liu atomizer.	(D’Alessio, Lazzaro, Massoli, Moccia, 1998)
FIBRE SUSPENDED DROPLETS		
Instituto Motori, Naples, Italy	Fibre-suspended droplets. Temperatures (673 – 1473 K). Atmospheric pressure. Initial droplet size (300-1000 µm). Air was used as carrier gas	(D’Alessio, Lazzaro, Massoli, Moccia, 1998)
Instituto Motori, Naples, Italy	Fibre-suspended droplets. Temperatures (300-1500 K). High pressure chamber (1-42 bars). Initial droplet size (400-1000 µm). Tests carried out in air.	Calabria, D’Alessio, Lazzaro, Massoli, Moccia (2000)
Dep. Mechanical Eng. Univ. of Ottawa	Fibre-suspended droplets. Temperatures (293-1073 K). Atmospheric pressure. Initial droplet size (1400- 1 800 µm). Tests carried in nitrogen and air.	Hallett, Clark, White, 2003)
THERMOGRAVIMETRIC TECHNIQUES		
Università di Pisa, Pisa, Italy	Thermogravimetric tests conducted at atmospheric pressure in air and nitrogen. Temperature (293-973 K)	(Vitolo, Ghetti, 1994)
Università degli Studi di Napoli, Italy	Thermogravimetric tests conducted at atmospheric pressure in air and nitrogen. Temperature (293-973 K)	(Branca, Di Blasi, Elefante, 2004)

Table 1: Bio-oil single combustion studies

Thermogravimetric testing can be considered as a first step in understanding a fuel’s evaporation and combustion characteristics. These tests are usually conducted at very low heating rates (usually between 1 and 30 °C/min) and, therefore, can only be used as an extreme reference in conditions where heat and mass transfer rates do not control evaporation and combustion. These tests are very important in the identification of phenomena controlled by fuel thermodynamics. Vitolo and Ghetti (1994) conducted thermogravimetric tests at 25 °C / min on bio-oils to a maximum temperature of 1000 °C. The researchers found that bio-oils in a nitrogen environment show two slopes in the

DTG curve. They attributed the first slope to the *evaporation of light fractions* and the second slope to the *cracking of heavy fractions (oligomers)*. The DTG curves for air showed that the *combustion of solid residue* occurs after 500 °C. Branca et al (2004) performed thermogravimetric tests in two steps. The first step targeted the evaporation and cracking under nitrogen (temperature up to 327 °C). In the second step the sample residue was heated to 600 °C in the presence of oxygen, in which case combustion occurred. A general conceptual mechanism applicable to combustion of bio-oils was proposed by the authors.

The main advantage of fibre-suspended droplet tests is that the measurement of droplet temperature is coupled with high-speed visualisation for determining changes in droplet diameters and morphology. The fibre-suspended droplet technique also makes it possible to study droplet combustion at relatively high pressures. Some of the disadvantages of the technique are that the minimum droplet size is limited by the fibre diameter and that it is hard to follow changes in mass. The presence of a fibre inside a droplet modifies their shape and may accelerate the nucleation of bubbles affecting a droplet temperature and morphology. Calabria et al. (2000) studied the combustion of fibre-suspended bio-oil droplets with diameters between 400 and 1100 µm in air pressures between 1 and 60 bars. The same three stages identified by thermogravimetric studies were also observed in the fibre-suspended droplet tests. At low pressures changes in droplet shape were observed. Calabria et al. (2000) found that the evaporation of very light compounds (primarily water) occurs at almost a constant temperature of around 130 °C. As the gradual *evaporation of light fractions* took place, droplet explosions and swelling reduced in frequency and intensity. When the temperature rose to 500 °C droplet explosions were completely absent and droplets appeared to contain a *large number of small bubbles*. The formation of stable flames that are initially blue in colour and are almost transparent occurs at around 600 °C. This step is characterized by an abrupt increase in temperature due to the large amount of heat transferred from the flame. Swelling and explosions resume and after they subside, the flame front settles at the maximum distance from the droplet surface (Calabria et al., 2000). The formation of a *yellow spot* follows indicating formation of soot (temperature around 650 °C). The flame shrinks towards the droplet

surface indicating the complete removal of volatile materials. In fact, immediately after the flame extinguishes, the *solid carbonaceous residue* starts to burn (temperature around 1097 °C) leading to the formation of ash. Similar results have also been reported by Hallet et al. (2003).

The fibre-suspended droplet method allows studying swelling at different pressures. This information is important for understanding fuel behaviour in Diesel engines that typically operate at pressures of up to 170 bars and in gas turbines engines that operate between 20 and 60 bars. The swelling reduces in intensity and completely disappears at pressures higher than 20 bars (Calabria et al., 2000) where the vapour pressure of the fuel volatile components is exceeded.

Entrained Flow Reactors ((EFR) are relatively sophisticated systems allowing the study of droplet combustion in very realistic laminar combustion environments (Shaddix and Hardesty, 1996, Wornat, Porter and Yang, 1994, D'Alessio et al, 1998). In these systems, the effects associated with the contact between solid surfaces and the droplets are eliminated. Bio-oil droplet combustion studies in EFRs were first conducted at Sandia Biomass Fuels Combustion System (BFCS) (Shaddix and Hardesty, 1996, Wornat, Porter and Yang, 1994, D'Alessio et al, 1998) under the following conditions: reactor temperature 1600 K, droplet diameters 320 µm and O₂ concentrations between 14 and 33 vol. %. The operating temperature was obtained using a laminar flow burner at the top of the reactor. The droplets were generated by the application of aerodynamic principles (droplet generation frequency used: 16 Hz). The main droplet combustion characteristics observed were the formation of more than one bubble inside the droplets that distorted the droplets shape and the occurrence of micro-explosions at the earliest evaporation stages.

The tests conducted by D'Alessio et al. (1998) were performed with droplet diameters between 10 and 40 µm generated by a Berglund-Liu droplet generator. The furnace worked at temperatures between 846 and 1300 K. The tests were conducted using blends of bio-oil in acetone (13.5 mass % of bio-oil) in order to reduce the bio-oil viscosity. The

solid residue formed presented two different morphologies: a) compact mechanically resistant spheres and b) fragile, glasslike cenospheres with thin walls (approximately 0.2 μm thickness).

The objective of this paper is to highlight, at a laboratory scale environment, the evaporation and combustion fundamentals of droplets of different pyrolysis oils. The sprays of SWBR derived bio-oils were used to identify the range of droplets sizes to be used in droplet evaporation studies. Bio-oil evaporation characteristics are studied under low heating rates by thermogravimetry and under relatively high heating rates with the CANMET Entrained Flow Reactor.

EXPERIMENTAL

Bio-oil Production and Characterization.

Two biomass feedstocks were used to produce the bio-oils investigated herein. The first feedstock was a softwood bark mixture originating from a pulp and paper plant debarking operation. This feedstock contained 75.9 mass % bark powder, 20.5 mass % wood fibres and 3.6 mass % cork. The feedstock was composed of three softwood species: 40 % white spruce (*Picea glauca*), 40 % balsam fir (*Abies balsamea*) and 20 % larch (*Larix laricinae*). In the present paper, this feedstock is called “softwood bark residue” (SWBR). The second feedstock contained less bark (34.6 mass %) and a higher amount of wood fibres (65.3 mass %) with almost no cork (less than 0.1 mass %). This feedstock originated from two hardwood species: approximately 70 mass % aspen poplar (*Populus spp.*) and 30 mass % white birch (*Betula papyrifera*). This material was called “hardwood rich in fibres” (HWRF). Both biomass feedstocks were pyrolyzed under vacuum (absolute pressures between 8 and 15 kPa) at 500 °C in two different reactors (laboratory and pilot reactors). The mass balance closures obtained for each feedstock are presented in Table 2.

Fraction	SWBR	HWRF
	Pilot plant (50 kg/h)	(15 L) Batch Lab. Reactor
Pyrolysis oils	25.0 (13.0 % water)	26.4 (13.0 % water)
Aqueous phase	20.0	27.5
Gas	27.4	19.9
Charcoal	27.6	26.2
Total	100	100

Table 2: Product Yields (mass %) Feedstock Anhydrous Basis, for the Vacuum Pyrolysis of SWBR and HWRF in two Different Reactors.

The SWBR derived bio-oil is an emulsion with droplets of 20 to 80 μm in size that contain waxy crystals dispersed in an oily matrix. The SWBR derived macro-emulsion can easily be separated (by decantation) into two phases after heating at 60 °C. The phase floating on top represents 16 mass % of the whole bio-oil and is called SWBR upper layer. The rest (84 mass %) is called SWBR bottom layer.

The HWRF bio-oil can be described as an oily matrix in which a small amount of waxy crystals are dispersed. This oil can be easily separated into two phases after heating to 60 °C. The lighter phase (1 mass %) has a waxy texture at 25 °C and is designated as HWRF waxy layer. The remaining bulky oily phase is called HWRF bottom layer. Table 3 presents some physico-chemical properties for the upper and bottom layers of the SWRB bio-oil and the bottom layer of the HWRF oil. A more detailed description of pyrolysis conditions used and bio-oil chemical composition can be found elsewhere (García-Pérez, 2004, 2005).

Properties	Units	SWRB (test H-67)		HWRF (tests G 823 – 830)
		Upper layer	Bottom layer	Bottom layer
Water content	mass %	3.5	14.6	13.0
Density (20 °C)	g/ mL ⁻¹	1.089	1.222	1.209
Kinematic viscosity	cSt			
at 50 °C		88	66	24
60 °C		50	38	16
70 °C		30	23	10
80 °C		21	15	7
90 °C		14	11	5
Gross Calorific Value (HHV) (dry basis)	MJ.kg ⁻¹	34.3	26.4	24.3
MIM (Methanol insoluble materials)	mass %	1.30	0.61	0.246
MeOH-CH ₂ Cl ₂ insolubles	mass %	0.28	0.58	0.095
Conradson carbon residue (CCR)	mass %	14.3	22.2	15.3
pH		3.03	2.98	2.34
Surface tension at 80 °C	(mN/m)	22.3	22.6	24.0
Elemental analysis	Mass % (on anhydrous basis)			
C		74.13	61.26	56.83
H		8.50	6.49	6.53
N		0.25	0.60	0.19
S		0.05	0.07	0.02
Ash		0.07	0.29	0.12
O (by difference)	17.00	31.29	36.31	

Table 3: Bio-oils Physico-Chemical Properties.

Thermogravimetric Analyses

An SSC/5200 TG/DTG (220) microbalance from Seiko was used for the thermogravimetric tests. The apparatus uses a horizontal differential balance mechanism. The samples were heated from room temperature to 750 °C at a rate of 10 °C/min in nitrogen and in air flows rate of 150 mL/min. A 10 mg sample was used in each test.

Bio-oil Atomization Installation

Bio-oils are heated to 80 °C and injected into an atomization chamber. A Malvern Master size analyser (2600 Series Particle Sizers) is used to measure the spray droplet size distribution. The results reported in this paper correspond to the atomization of SWBR whole bio-oil in a Delavan nozzle (type A, nominal spray angle of 70°, Flow number: $5.51 \cdot 10^{-8} \text{ m}^2$). A detailed description of the experimental set up used to study bio-oil sprays can be found elsewhere (García-Pérez et al, 2004).

Entrained Flow Reactor

The evaporation of SWBR and HWRF derived oils droplets was conducted at the CANMET Entrained Flow Reactor (EFR). A schematic of this installation is shown in Figure 1. The centrepiece of this facility is a high-temperature laminar flow reactor into which a steady stream of separate droplets is injected. This furnace is designed to subject the material under study to a high radiant flux. The droplets are introduced into the EFR by means of the burner (1). The burner (ID 12.36 mm, length 1000 mm) is designed in such a way that the laminar gas stream carrying the droplet enters the EFR along the centre line of the furnace without touching the walls. The burner head is also used to remove the solvent (methanol) that was introduced into the bio-oil (50 % vol.) to generate the droplets. A dried primary gas (3.63 L/min of Ar or Ar-O₂ mixtures at ambient temperature and pressure) is introduced into the burner central tube (1) allowing the formation of a laminar flow necessary to ensure the drying and transport of a droplet before it enters the furnace.

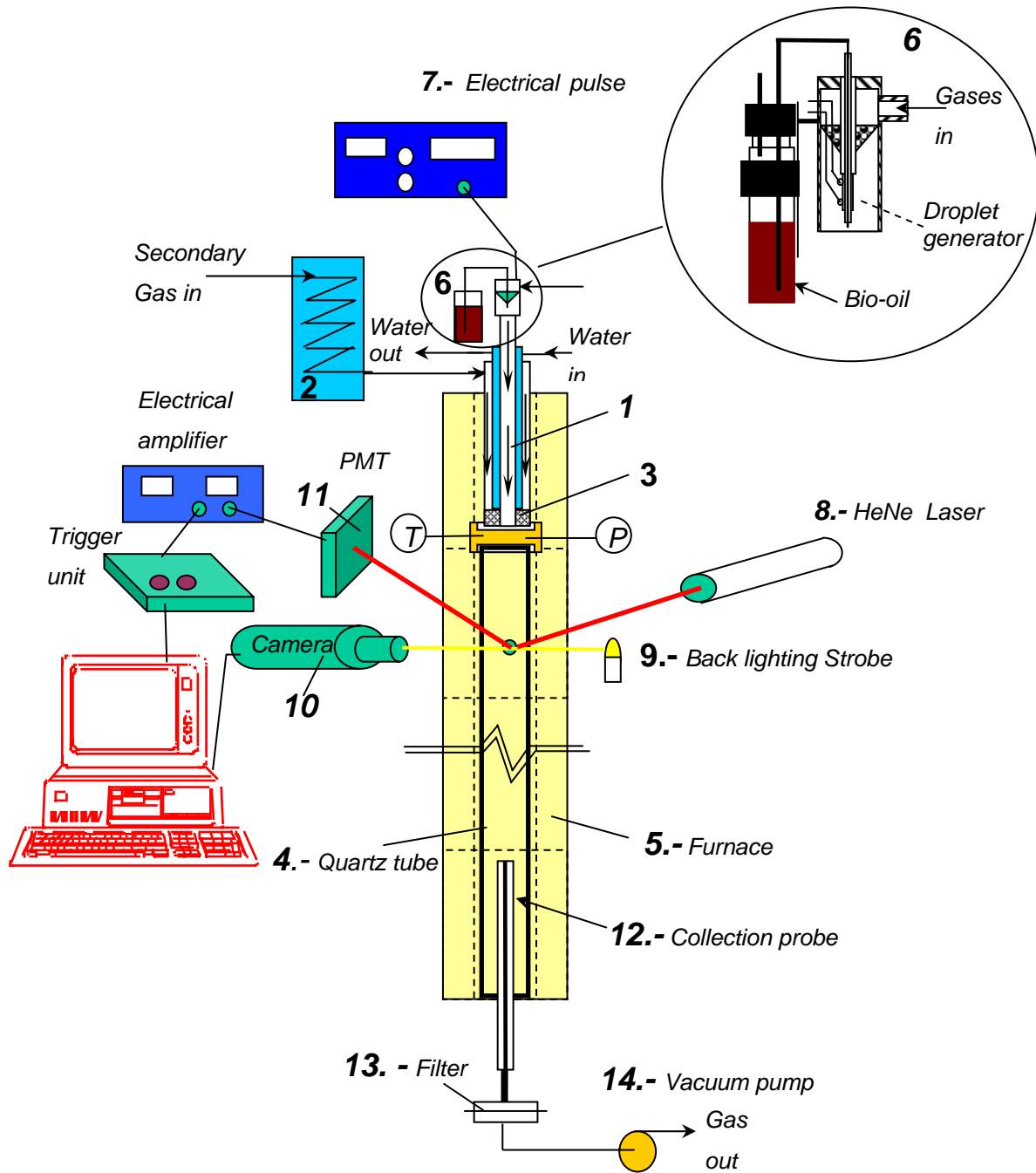


Figure 1. Schematic of CANMET's Entrained Flow Reactor

A coolant jacket is placed around the central tube carrying the primary gas to ensure that the droplets remain cold enough (less than 35 °C) to avoid the occurrence of reactions before entering the EFR. A secondary or annular gas flow of 13.59 L/min at ambient temperature and pressure also enters the EFR through the burner. This annular gas flow

has been heated to 180 °C by an electrical heater (2) before entering the furnace. At the EFR entrance, the annular gas encounters a ceramic honeycomb (3) to straighten the flow. The primary flow containing the droplet is constrained to flow down the centre of the EFR's quartz tube (ID 70.00 mm; length 1.55 m) (4) by appropriate adjustment of the primary and secondary gas flow rates and the level of suction of the vacuum pump (14).

The reactor quartz tube is heated by 64 glow bars (32 on each side). The furnace (5) is divided into four zones whose temperatures are maintained by four separate controllers. If needed, this configuration permits zones of different temperatures, in order to simulate temperature gradients observed in some real combustion systems. During the current experiments, two wall temperatures were used for all the zones: 700 and 800 °C.

Each bio-oil studied was blended with (50 vol. %) methanol in order to reduce its viscosity. The mixture was then filtered using a 0.2 µm filter before being introduced into the droplet generator. These operations were needed to avoid the clogging of droplet generator nozzles. The droplets were produced by using a piezo-electric generator (6) that has a glass tube nozzle with a precise shape and a sharp break-off edge (Ulmke, Wriedt and Bauckhage, 2001). Each time a droplet was generated, a pressure wave was produced through the nozzle causing a droplet ejection speed of around 2 m/s. In these conditions, the droplets were expected to attain the same velocity as the surrounding laminar gas flow. The droplet generation frequency was dictated by the electrical pulse frequency (7). The experiments were conducted at frequencies between 50 and 500 Hz using 60 µs pulses of 87.2 Volts. For this range of frequencies, good reproducibility of droplet evaporation was observed. At higher frequencies it was not possible to obtain reproducible results. Tests at 100 and 50 Hz were always conducted to confirm the independence of droplet evaporation on generation frequency.

Imaging of the evaporating droplet was performed by simultaneously triggering (8) a back-lighting strobe (9) and a high 'shutter-speed' digital camera (10). The trigger signal was generated by a PMT (Photomultiplier Tube) that detected scattered light when the droplet crossed a strategically positioned laser beam. The optics were mounted on

platforms affixed to the furnace structure. The optical system was able to image droplets up to 1 m downstream from the burner face. Droplet diameters at a given measurement location were determined by measuring the projected droplet area assuming sphericity. Typically 15 individual measurements were averaged. The camera was calibrated with a wire of known diameter (500 μm) that was placed inside the furnace. The time difference between the moment at which the droplet generator was turned off and the moment when the PMT (11) did not detect the presence of any droplets was used to estimate the residence times.

In addition to the pictures taken of the stroboscopically backlit droplets, other sources of information were used, including a collection probe (12) that allowed solid particles to be collected. The sampled material travelled down the sample probe and the particulate was removed using a filter paper (13). Samples collected in this way were analysed by Scanning Electron Microscopy (SEM).

RESULTS AND DISCUSSION

Thermogravimetric Studies

Figure 2 shows the TG and DTG (differential TG) curves obtained for SWBR bio-oil (bottom and upper layer) and for HWRF bio-oil (bottom layer) in nitrogen and in air. It is evident from the figure that bio-oil combustion occurs in three major steps. The first step corresponds to the evaporation of light compounds (from 25 °C to 280- 320 °C) (see the tests conducted under N_2). The pyrolysis of heavy fractions (oligomers) between 320 and 480 °C follows. The final step, which is characterised by the spike in the DTG curves, is associated with the attack of O_2 on the carbonaceous solid residue formed following the first two steps.

In the temperature range from 200 and 300 °C, there are important differences in the evaporation and cracking behaviour between TG in nitrogen and TG in air. The differences can be explained by the absorption and reaction of oxygen with bio-oils. The

oxygen seems to intervene in polymerization reactions leading to the formation of extra char. This phenomenon is observed in the same range of temperatures at which the pyrolysis of sugars occurs (García-Pérez, 2005) suggesting that the oxygen presumably stabilizes the structure of sugars and reduces their tendency to pyrolyse and form volatile compounds.

It is worthy to note that the absorption of oxygen in bio-oil droplets is a process that depends on i) the rate of oxygen diffusion in the vapour phase, ii) of the absorption of oxygen by the bio-oil (determined by phase equilibrium), iii) diffusion of oxygen in the liquid phase and of the oxygen reaction rates. If the polymerization rate (reaction involving oxygen) is very high compared with the diffusion of oxygen in the liquid phase, then a surface polymerization reaction leading to the formation of a skin occurs. This skin could inhibit evaporation from the droplet interior. If the reaction rate is very slow compared with the diffusion of oxygen in the liquid phase, then the polymerization occurs in whole droplet volume. There is a competition between the polymerization reactions consuming oxygen and leading to the formation of a carbonaceous residue and the cracking reactions leading to the formation of volatile compounds. The rate of removal of these volatile compounds depends on mass transfer rates within the droplets.

Higher heating rates will have a direct effect on the increase of droplet temperatures. The impact of this increase on chemical reactions (polymerization and cracking reactions) will depend on the activation energy of each reaction. Usually the temperatures have a more moderate effect on the diffusion coefficients. Less carbonaceous residues form at high heating rate if the activation energy corresponding to the cracking reactions leading to the formation of volatile compounds is higher than the one corresponding to polymerization reactions leading to the formation of carbonaceous residues.

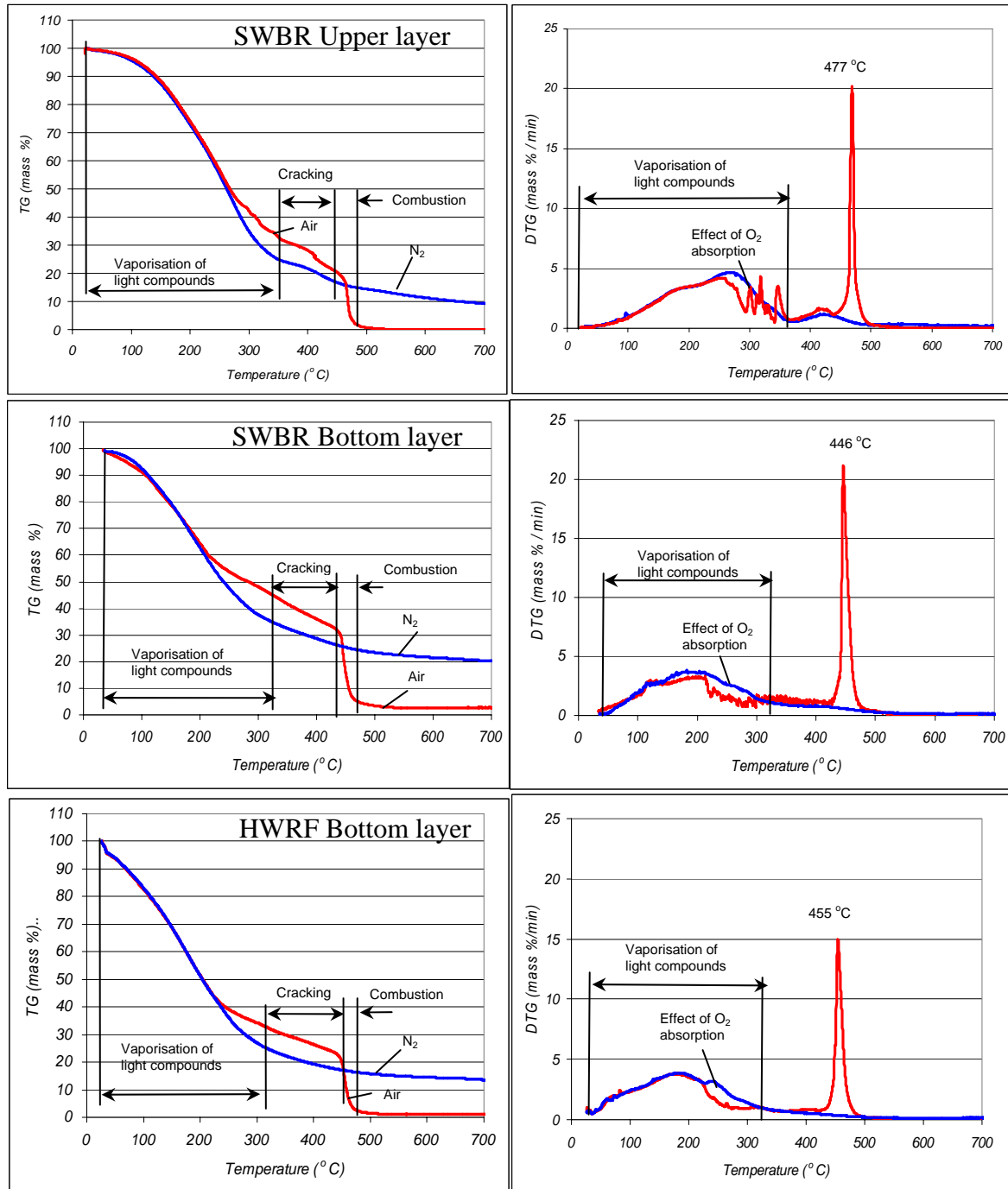


Figure 2: TG and DTG Curves for 3 Different Bio-oils in Air and in Nitrogen.

There are certain differences in the evaporation and pyrolysis temperature range between observations of fibre-suspended droplets (D'Alessio et al, 1998, Calabria R et al., 2000, Hallet, Clark, White, 2003) and the present TG observations. In general the evaporation and pyrolysis phase observed in fibre-suspended droplets is shifted to higher

temperatures, indicating certain delays associated with mass transfer limitations for high heating rates.

The solid residue formed after the removal of volatile materials in the presence of oxygen represents (at around 450 °C), 32, 20 and 25 % of the initial mass of SWBR bottom layer, SWBR upper layer and HWRF bottom layer respectively. The solid residue remaining at 700 °C in the presence of nitrogen were 20, 10 and 15 % of the initial mass of SWBR bottom layer, SWBR upper layer and HWRF bottom layer, respectively. These values are very near to the Conradson carbon residue (CCR) determined for each of these oils (see Table 3). As expected the SWBR upper layer is the oil with a lower tendency to form carbonaceous residues due to the larger content of hydrocarbon-like compounds. For the TG experiments in air, the range of temperatures in which the attack of oxygen occurs is between 455-477 °C. This temperature range is very close to the one reported by Branca et al. (2004) for other bio-oils. The position of the peak reported for the “Pyrovac derived char” (456 °C) (Branca et al, 2004) was very close to the one measured here for the SWBR bottom layer (455 °C) because both oils were obtained from the same feedstock and technology. Branca et al. (2004) classified the carbonaceous residue for this bio-oil as the most reactive of all studied bio-oils.

Spray Characterization of SWBR-Derived Bio-oil

The fineness of an atomization process is usually described in terms of the Mean Sauter Diameter (SMD). The SMD is the diameter of a representative drop whose ratio of volume to surface area is the same as that of the entire spray. Figure 3 presents the behaviour of SMD at different pressure drops for water, heating oil and SWBR whole bio-oil at 80 °C. The used atomizer (Delavan Type A, $FN= 5.51 \cdot 10^{-8} \text{ m}^2$) is able to provide SMD values as low as 45 μm using bio-oils. For the realistic feeding pressures shown, the SMD values obtained varied between 77 and 45 μm . The SMD values of SWBR bio-oil sprays are larger than those observed for water and heating oils. This result can be attributed to the bio-oil higher viscosity.

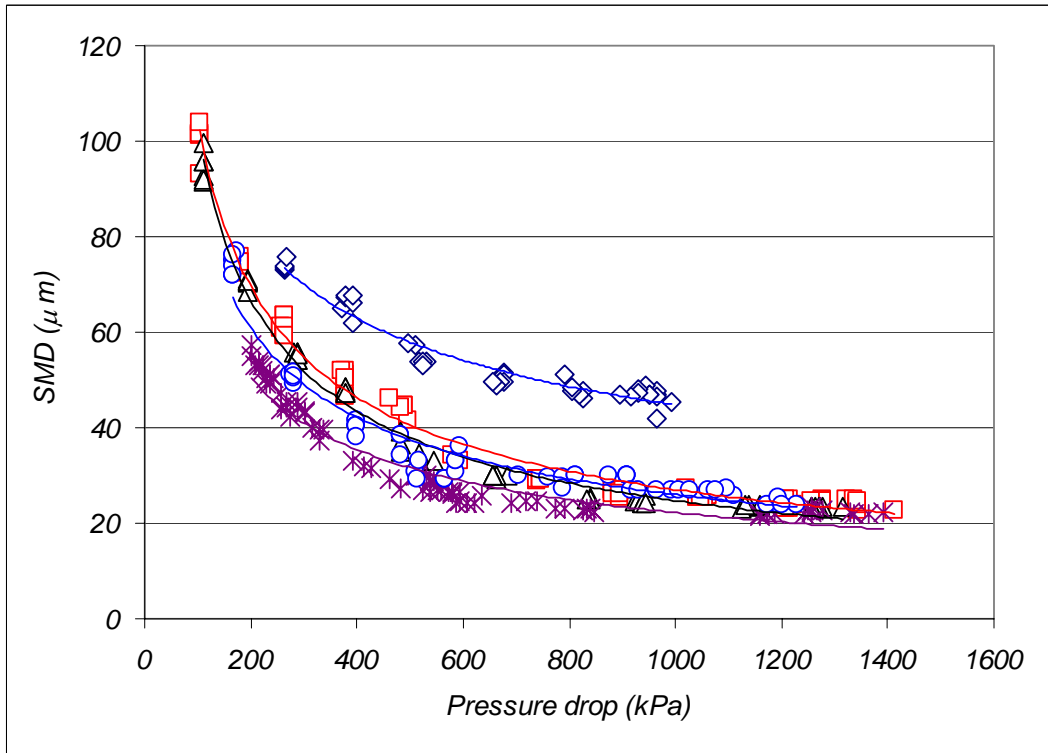


Figure 3: SMD vs. Pressure drop for a Delavan atomizer (Type A, $FN = 5.51 \cdot 10^{-8} \text{ m}^2$).

Figure 4 shows droplet size distribution of bio-oil sprays at different feed pressure.

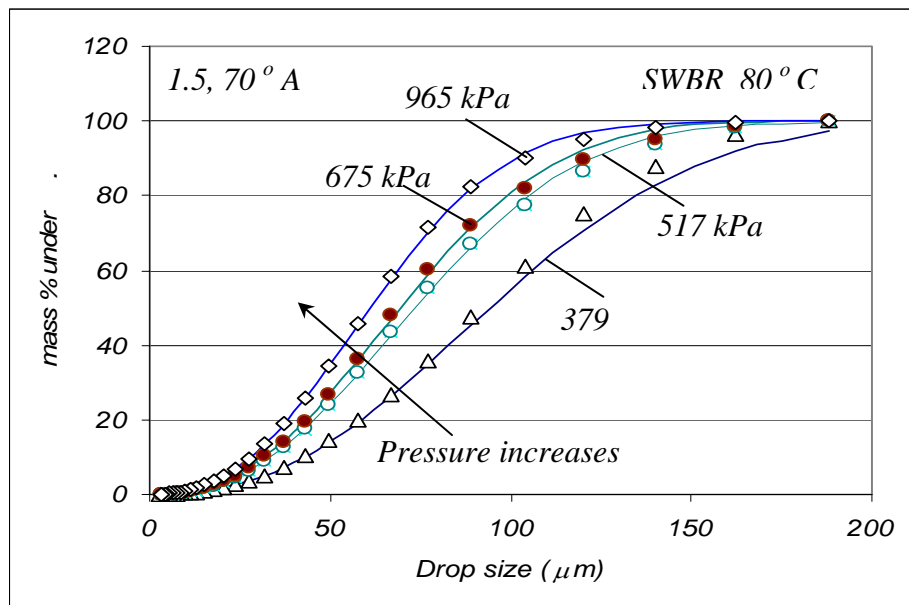


Figure 4: Bio-oil Droplet Size Distribution at Different Feeding Pressures using a Delavan Nozzle (Type A, $FN= 5.51 \cdot 10^{-8} \text{ m}^2$).

Droplets generated with these sprays can vary from a few microns to more than 150 μm . Based on these results; a representative initial droplet size of 60 μm was chosen to study the evaporation behaviour of bio-oil droplets.

Droplet Evaporation in the EFR

The initial droplet diameter obtained using the piezoelectric droplet generator (nozzle N° 36) was 74 μm . Frequencies between 50 and 500 Hz were used in the experiments. These frequencies correspond to droplet spacing comprised between 0.04 and 0.004 m (or droplet-spacing to droplet diameter ratios of between 540 and 54). Ratios over 50 are necessary to eliminate any potential interaction during combustion of successive droplets. Bio-oils were blended with 50 vol. % of MeOH to allow the formation of small droplets. Ideally all the methanol must be removed before the droplets enter the furnace. The initial droplet size measured at the furnace entrance was 62, 54 and 58 μm for SWBR bottom layer, SWBR upper layer and HWRF oil, respectively. These values are very close to the ones expected ($0.5^{0.33} * 74 = 58.76 \mu\text{m}$) if one assumes that all the methanol added is removed in the burner central tube. The observed differences can be explained by the experimental uncertainty in droplet size measurements.

Figure 5 presents the evolution of bio-oil droplet sizes at different residence times for two EFR wall temperatures. The measurements in Figure 5 include droplet diameters measured when bubbling was occurring.

At wall temperatures of 700 °C, the slope of the diameter vs. time curves is very small for the first 150 ms. This behaviour can be explained by the fact that most of the heat transferred to the droplet from the EFR walls is used to heat the droplet with no evaporation occurring. According to Chin and Lefebvre (1985), this heating period is commonly proportional to the square of the fuel droplet diameter. The heating period increases for higher pressures and decreases with lower heating rates and initial droplet temperatures.

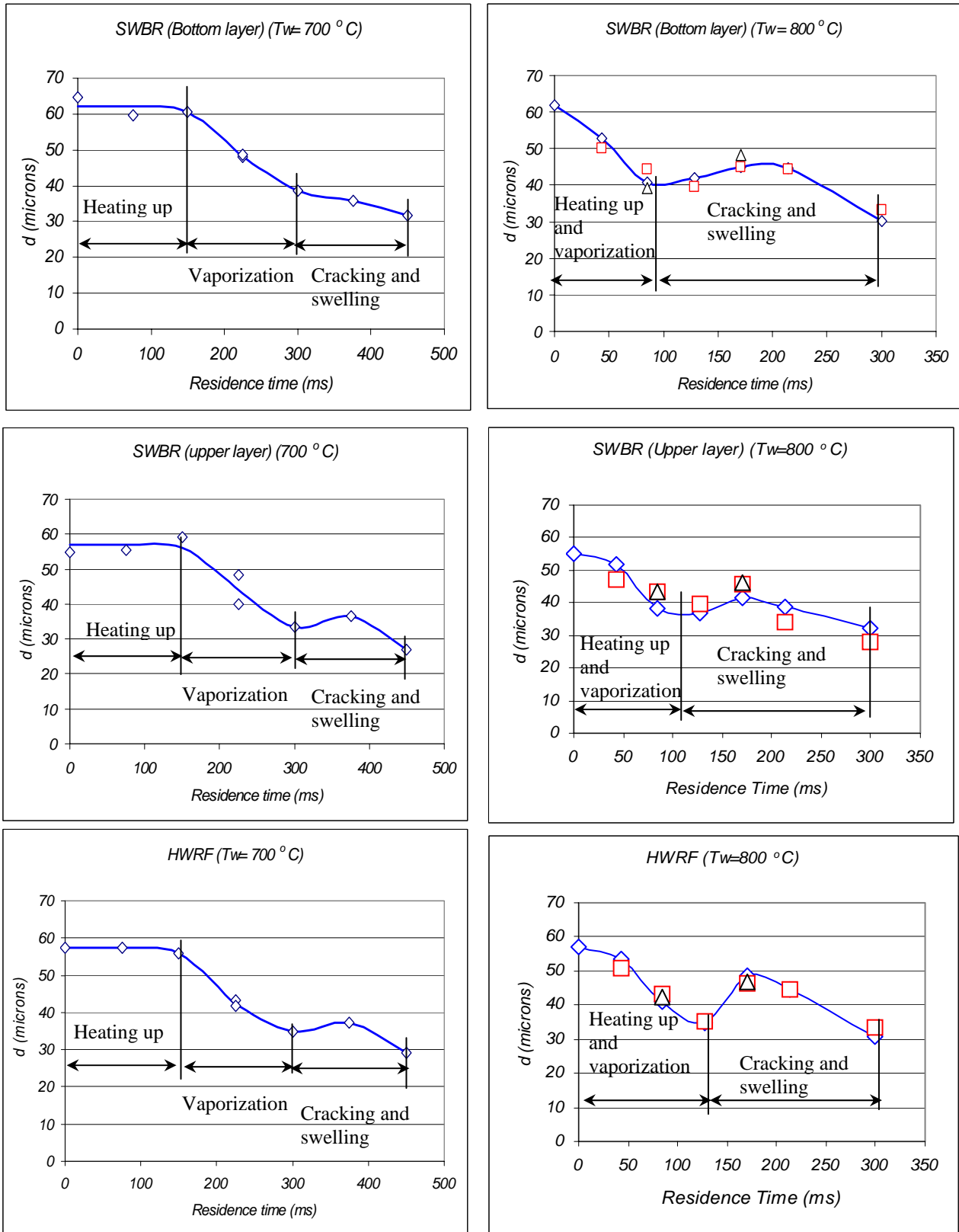


Figure 5: Droplet Size at Different Residence Time in the EFR at two Wall Temperatures.
 \diamond In Argon, \square 20 vol. % Oxygen, \triangle 50 vol. % Oxygen.

In the second stage, a rapid decrease in droplet diameter corresponding to the evaporation of light compounds occurs. This step can be observed between 150 and 300 ms. At a certain point, the droplets start to swell presumably due to the formation of small bubbles inside. The enrichment in heavier compounds due to depletion of lighter species and liquid phase polymerization can be deemed responsible for an increase of viscosity and the formation of a skin whilst temperature increases (Calabria et al., 2000). The formation of bubbles inside droplets exposed to high heating rates has been reported for many other multicomponent liquids (Wornat, Porter and Yang, 1994).

High values of Peclet (Pe) (ratio between the droplet external convective and internal diffusive mass transfer) and Lewis (Le) (ratio between droplet thermal and mass diffusivities) are usually observed in fuels with high viscosity (high molecular mass) and in systems with relatively low velocities between the droplets and the surrounding environment. In these conditions the droplets present minimal internal circulation. For these fuels the mass transfer within the liquid phase is very slow. As a consequence, the composition of droplet surfaces get enriched in heavy fractions as the evaporation of volatile fractions from the surface cannot be compensated by the migration from the droplet core. The enrichment in heavy compounds and the faster polymerization reactions rate near the surface are likely to contribute to the formation of a film with increasingly viscoelastic properties as temperature increases. At high heating rates the droplet core reaches temperatures high enough to form vapours by the evaporation of light fractions or by cracking of heavy oligomers. Since these vapours cannot reach the surface they are constrained to nucleate forming vapour bubbles within the droplet. The nucleation of bubbles inside the droplet is accelerated by the presence of solid surfaces, for example char particles (Wornat, Porter and Yang, 1994). Swelling of the vapour-filled droplet occurs until the internal pressure developed by the vapours overcomes the combustion chamber pressure, the surface tension forces and the skin formed holding the droplet together. From time to time the vapours can escape from the droplets after breaking the weakest part of the film. Micro-explosions leading to droplet fragmentation can occur if the swelling rate is very high. In some cases a new droplet is formed after the escape of vapours due to the action of surface tension. In cases where the film is exposed to high

heating rates a rigid carbonaceous film can be formed. The film could be rigid enough to halt the droplet shrinkage. In the experimental conditions used in the present study, the vapours formed inside the droplets escape without fragmenting the droplets. Droplets subsequently shrink under the effect of surface tension leading to the formation of carbonaceous residues.

Comparative evaporation tests were conducted by Lappas et al. (2004) using Fuel N° 2 in the same installations and under the same experimental conditions (wall temperatures of 700 °C, initial droplet Fuel N° 2 diameter 68 µm). A very similar heating period was obtained for Fuel N°2 and bio-oils (around 177 ms). This first step was followed by a steady state evaporation of fuel compounds that ended at approximately 220 ms. The lifetime of Fuel N° 2 droplets is very small compared to bio-oils. The evaporation constant obtained was 1.09 mm²/s.

As shown in Figure 5, the evaporation behaviour of the bio-oil droplets at 800 °C was different to that observed at 700 °C. The differences can be explained by the increased heating rates at 800 °C. The initial heating up period is considerably reduced, to the point that it is not well detected. The evaporation of light compounds is observed at smaller residence times. The droplet swelling is more pronounced indicating larger amounts of vapour trapped inside the droplets. Droplet shape remains near spherical in all experiments indicating that only one bubble is formed inside the droplets. The increase in the ratio between the heat and mass transfer rates explain the trapping of larger amounts of vapour at higher heating rates. The three bio-oils investigated exhibit quite similar evaporation features. The largest tendency to swell is observed for the HWRF derived oil. This oil presents the lower molar mass of all the studied oils. The differences in chemical composition found in these oils (García-Pérez et al., 2005) do not seem to significantly affect the overall evaporation behaviour of bio-oil droplets.

Contrary to the experimental evidence reported in fibre suspended droplets and in hot plate combustion tests, the formation of any flame surrounding the droplets was not observed in the present study. Neither visible flame nor a measurable effect of oxygen

presence on the droplet size evolution was observed. The organic vapours evolving from the single tiny droplets studied did not reach a concentration high enough to sustain a flame. The absence of a flame can also be due to the existence of important heat losses toward the surrounding environment at relatively low temperature compared to the droplet. The droplet is mainly heated by radiation, while the surrounding gas is mainly heated by conduction from the EFR walls.

It seems that the temperature reached by carbonaceous residues in the range of residence time studied were not high enough (more than 450 °C) to allow the attack by oxygen. It is also possible that the diffusion of oxygen to the char surface in laminar conditions was not high enough. In fact, no difference in diameter was observed when the concentration of oxygen was increased up to 50 vol. %. This result cannot be considered a definitive proof but it is a preliminary indication that the presence of oxygen does not modify the evaporation features of bio-oils undergoing relatively high heating rates.

Bio-oil droplet evaporation tests reported in the literature (Shaddix and Tennison, 1998, Wornat, Porter and Yang, 1994) using larger droplets (320 µm) and higher heat transfer rates (surrounding environment 1600 K) show a more dramatic deformation in droplet shape than that found in this study. The formation of multiple bubbles inside droplets is a direct result of considerably larger droplet diameters. In these conditions micro-explosions ensue.

Analysis of Bio-oil Evaporation Residues

Figure 6 shows pictures obtained by Scanning Electronic Microscopy (SEM) of solid residues in the tests carried out at 700 °C. The left hand side shows the solid residue obtained when the droplet generator was operated at frequencies smaller than 500 Hz.

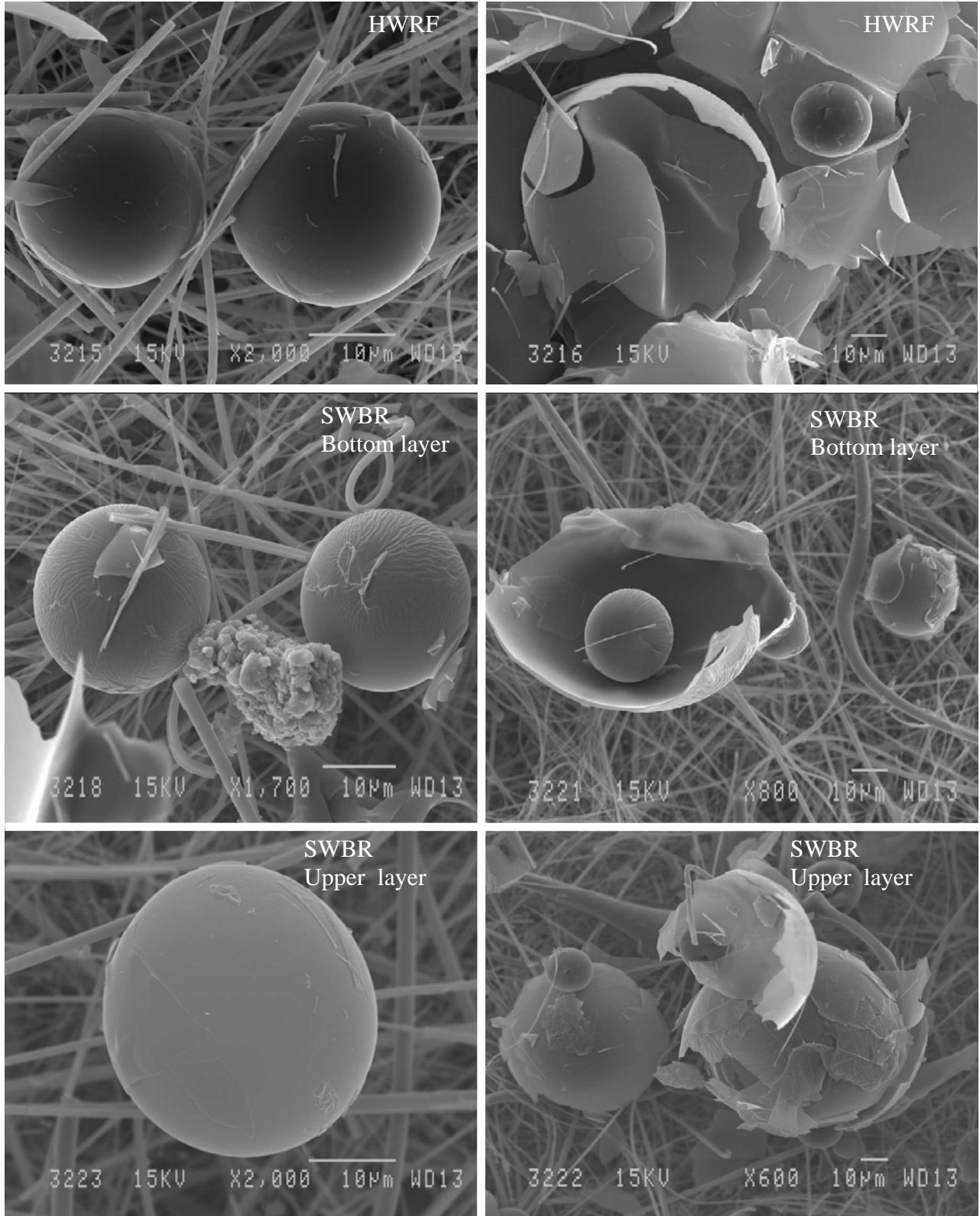


Figure 6: Scanning Electron Micrograph of Solid Produced from HWRP, SWBR (Bottom and Upper Layer).

The right hand side (Figure 6) shows the results for tests in which the droplet generator operated at frequencies between 500 Hz (droplet spacing to droplet diameter larger of 54) and 1000 Hz (droplet spacing to droplet diameter of 27). Comparison of the two sides indicates that two different morphologies of residual particles exit the EFR depending on the frequency: a) more compact mechanically resistant spheres obtained at low frequencies (less than 500 Hz) with a typical diameter of 20-25 μm and b) fragile glass “like” cenospheres with thin walls and menisci with a diameter between 60 and 90 μm obtained at higher frequencies (1000 Hz). This phenomenon can be explained by assuming that, at higher frequencies, the methanol added to bio-oil droplets is not completely removed before entering the EFR. The methanol vapour from neighbouring droplet could affect methanol evaporation events if the droplet spacing to droplet diameter is smaller than 50. The fuel mass flow added to the reactor increase proportionally to the feeding frequency. This highly volatile species will contribute to the formation of a relatively large bubble inside each droplet. Bio-oil heavy compounds will form on the bubble thin walls after polymerization. The use of higher frequencies increased the net amount of bio-oil fed to the central tube burner. In these conditions, the concentration of methanol surrounding the droplets increased, reducing the methanol mass transfer rate between the droplets and the surrounding environment. In an extreme case, the surrounding environment can reach methanol saturation, effectively stopping the further removal of methanol from the droplets in the burner.

Similar results are reported by D'Alessio et al. (1998), however the solid residues collected were slightly bigger (100-200 μm) than the one obtained in this study. The surface of the carbonaceous residues was generally smooth. Branca et al. (2004) have compared the reactivity of carbonaceous residues from bio-oil with the reactivity of wood char. They suggested that the higher reactivity of biomass char compared with bio-oil carbonaceous residue can be explained by accounting for the heterogeneous nature of combustion reactions and the highly micro-porous structure of wood char. The non-porous surface of bio-oil residue has a relatively small area for attack by oxygen. In turn, this increases the overall particle combustion time.

The diameter of residue spheres (between 20 and 25 μm) measured by SEM is slightly smaller than the droplet diameter measured at 450 ms (around 30 μm) with the camera images for the three oils. Assuming that the droplet temperature at the oven exit is high enough to allow the removal of all the volatile materials (as determined by the thermogravimetric studies under nitrogen) and that the bio-oil density is the same as the char density, the droplet size at the EFR exit should be calculated as follows: $0.2^{0.33} * 62 = 36.25 \mu\text{m}$ for SWBR Bottom layer, $0.10^{0.33} * 54 = 25.01 \mu\text{m}$ for the SWBR upper layer and $0.15^{0.33} * 58 \mu\text{m} = 30.81 \mu\text{m}$ for the HWRF. The values calculated are slightly higher than the ones measured by SEM. These differences are explained not only by the higher density of the char originating from the removal of volatile fractions but also by the polymerization and cracking of heavy fractions in bio-oils. Some small systematic errors associated with the measurement of particle sizes can explain part of the observed discrepancies. Another hypothesis could be that the degree of polymerization reactions at high heating rates is smaller than that observed in thermogravimetric analysis, thus reducing the amount of solid residue formed after the removal of volatiles.

CONCLUSIONS

Thermogravimetric analyses of bio-oils in N_2 and in air show the presence of three clear steps in bio-oils combustion. In the first step (up to 300 $^\circ\text{C}$), the *evaporation of light fractions* occurs while above 300 $^\circ\text{C}$ the *cracking of heavy fractions* occurs. The TG curves of bio-oil in the presence of air show that the *combustion of solid residue* finally occurs between 400 and 500 $^\circ\text{C}$ (third step). At low heating rates, the oxidation of bio-oils liquid compounds occurs. The droplets analyzed in the EFR system were in the range of droplet sizes observed in typical bio-oil sprays. In the EFR, the same steps as those for low heating rates were observed. Nevertheless, the diameter of bio-oil droplets increases due to the formation of vapor bubbles inside them. This phenomenon is more pronounced as heating rates increase. No change in droplet spherical form was observed. Bio-oil droplet lifetime is considerably larger than that for Fuel N^o 2.

The small droplet diameters (60 μm) and the relatively low heating rates (environment temperatures 700-800 $^{\circ}\text{C}$) used in this study represent the opposite extreme of the conditions used in the Sandia experiments (droplet sizes of 320 μm and environment temperatures of 1327 $^{\circ}\text{C}$). Since larger bio-oil droplets tend to micro-explode during low pressure combustion while smaller ones do not, a wide range of droplet morphologies is expected in most practical applications.

ACKNOWLEDGEMENTS

The authors gratefully acknowledge NSERC, la Fondation de l'Université Laval and CANMET for financial support for this project. The authors are also very thankful to Myles Legere, Abdel Iris, Doug Percy, Richard Lacelle and Alan Vaillancourt for their contribution in the conception, construction and operation of CANMET EFR installation.

REFERENCES:

Beer J. M., Lewis P, Shihadeh A, Manurung R (1994). Combustion Characterization of Biomass Oils. Combustion Research Facility. MIT, Energy Laboratory, Cambridge, Ma. August.

Branca C., Di Blasi C., Elefante R. (2004). Controlled Temperature Combustion of Wood Fast Pyrolysis Oils. Accepted in *Industrial and Engineering Chemical Research*.

Calabria R., D'Alessio J., Lazzaro M., Massoli P., Moccia V. (2000). Bio-fuel oil. Upgrading by Hot Filtration and Novel Physical Methods. Task 5: Fundamental Behaviour of BFO in Combustion. Contract: JOR3-CT97-0253. Final Report, December. Research funded in part by: The European Commission in the framework of the Non Nuclear Energy Programme Joule III

Chin J.S., Lefebvre A.H. (1985). The Role of the Heat up Period in Fuel Drop Evaporation. *International Journal of Turbo and Jet Engines* 2, pp. 315-325.

Czernik S., Bridgwater A.V. (2004) Overview of Application of Biomass Fast Pyrolysis Oil. *Energy & Fuel*, 18 (2) pp. 590-598.

García-Pérez M., A. Chaala, H. Pakdel, D. Kretschmer, P. Hughes, C. Roy (2004) The Complex Structure of Bio-Oils. In Proceedings of 2nd World Conference on Biomass for Energy, Industry and Climate Protection. Rome, Italy, May 10-14 (In Press)

García-Pérez M, A. Chaala, D. Kretschmer, A. De Champlain, P. Hughes, C. Roy (2004) Spray Characterization of a Softwood Bark Vacuum Pyrolysis Oils. In Proceedings of Science in Thermal and Chemical Biomass Conversion, Victoria, Vancouver Island, BC, Canada, 30 August-2 September (In Press).

García-Pérez M. (2005). Fuel Properties of Vacuum Pyrolysis Oils Derived from Wood Industry Residues. Ph.D. Thesis. Université Laval.

Hallett W.L.H, Clark N.A. (2005) A Model for the Evaporation of Biomass Pyrolysis Oil Droplets. *Fuel*, 85, pp. 532-544.

Lappas P, Garcia M, Dell L, Derome S, Faguy D, Hughes P, Iris A., Lacelle R., Legere M., Percy D., Vaillancourt A. (2004) Photographic Determination of Devolatilization & Combustion Rates of Liquid Bio-fuel Droplets. Presented In: Sciences in Thermal and Chemical Biomass Conversion. Victoria, Vancouver Island, BC, Canada, 30 August -2 September.

Shaddix C.R., Hardesty D.R. (1996). Combustion of Biomass Flash Pyrolysis Oils. Final Project Report. Combustion Research Facility. Sandia National Laboratories. Livermore. CA.

Shaddix C., Tennison P. (1998). Effects of Char Content and Simple Additive on Biomass Pyrolysis Oil Droplet Combustion. *Twenty-Seventh Symposium (International) on Combustion* / The Combustion Institute, p. 1907-1914.

Ulmke H, Wriedt T, Bauckhage K. (2001). Piezoelectric Droplet Generator for the Calibration of Particle-Sizing Instruments. *Chem. Eng. Technol.* 24, 3. p. 265-268

Vitolo S., Ghetti P. (1994) Physical and Combustion Characterization of Pyrolytic Oils Derived from Biomass Material Upgraded by Catalysis Hydrogenation. Short communication. *Fuel*, 73, N° 11, p. 1810-1812.

Wornat M. J., Porter B. G., Yang N. Y. C. (1994). Single Droplet Combustion of Biomass Pyrolysis Oils. *Energy and Fuels*, 8, 1131-1142.

D'Alessio J., Lazzaro M., Massoli P., Moccia V. (1998). Thermo-optical Investigation of Burning Biomass Pyrolysis Oil Droplets. Twenty-seventh Symposium (International) on Combustion/The Combustion Institute. pp. 1915-1922.